

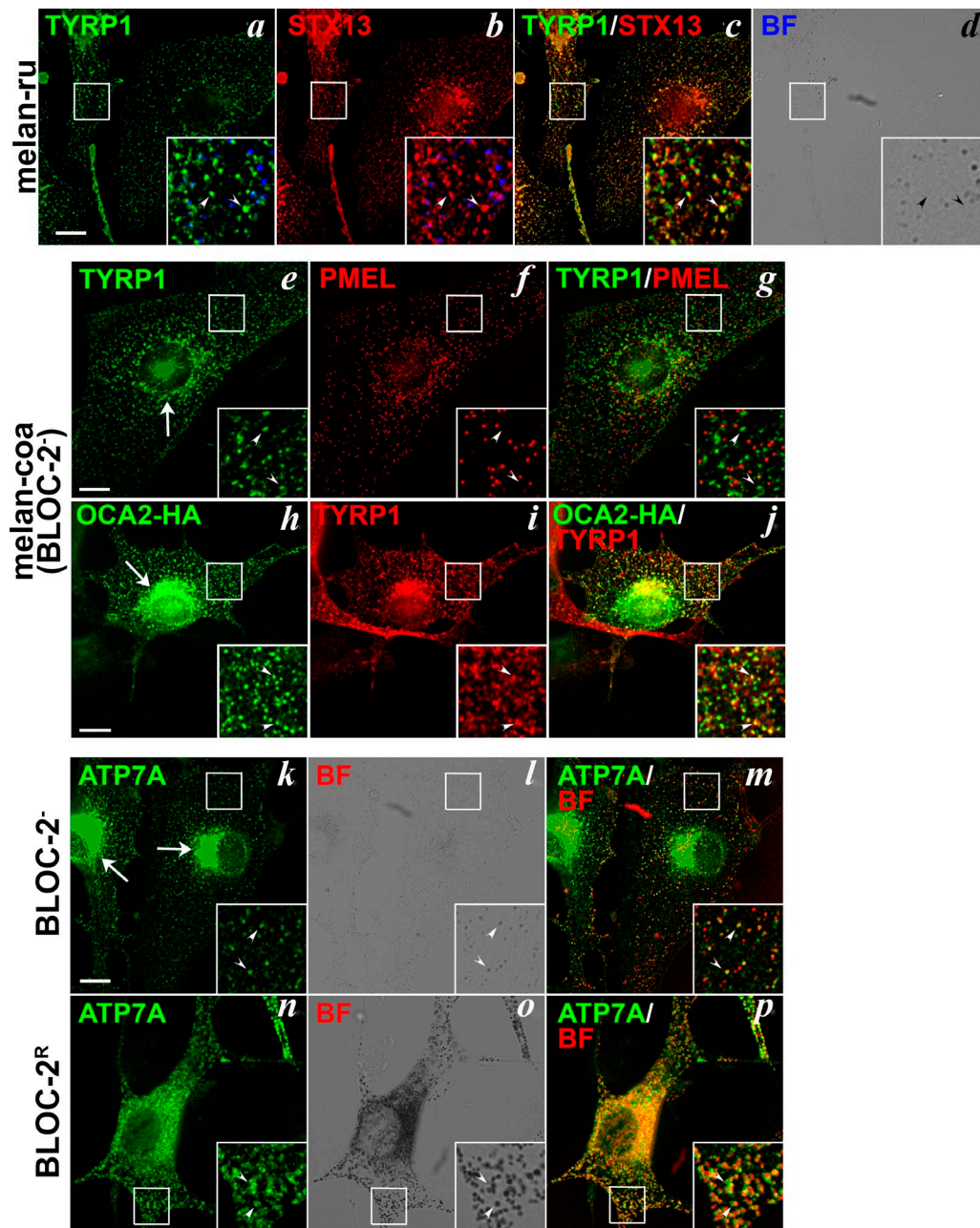
Dennis et al., <http://www.jcb.org/cgi/content/full/jcb.201410026/DC1>

Figure S1. **TYRP1 and ATP7A localization in BLOC-2-deficient melanocytes.** Fixed cells were analyzed by deconvolution IFM. (a–d) Melan-ru cells, derived from HPS6-deficient *ruby* eye mice, were labeled with antibodies to TYRP1 (a) and STX13 (b). (c) Merged image. (d) Corresponding bright-field (BF) image. Insets, 3× magnification of boxed region showing overlap of TYRP1 with bright-field (BF; a), STX13 with bright-field (b), TYRP1 with STX13 (c), or bright-field alone (d); pigment granules are pseudocolored blue for overlap. Arrowheads indicate examples of overlap between TYRP1 and STX13. (e–g) BLOC-2⁻ melan-coa cells were labeled for TYRP1 (e, green) and PMEL (f, red). (g) Merged image. Insets, 3× magnification of boxed region. Arrowheads indicate examples of TYRP1 labeling lacking PMEL. Large arrow in e indicates perinuclear accumulation of TYRP1 in BLOC-2⁻ cells. (h–j) BLOC-2⁻ melan-coa cells were transfected to express OCA2 with a luminal HA tag 24 h before fixation. Cells were labeled for HA (h) and TYRP1 (i). (j) Merged image. Insets, 3× magnification of boxed region. Arrowheads indicate examples of OCA2 overlap with TYRP1. Large arrow in h indicates perinuclear accumulation of OCA2 in BLOC-2⁻ cells. (k–p) BLOC-2⁻ melan-coa (k–m) or rescued BLOC-2^R cells (n–p) were labeled for ATP7A (k and n) and analyzed in parallel by bright-field analysis [BF; l and o]. (m and p) Merged images in which pigment granules are pseudocolored red. Insets, 3× magnification of boxed region. Arrowheads indicate examples of overlap between ATP7A and pigment granules. Large arrows in k indicate perinuclear accumulation of ATP7A in BLOC-2⁻ cells. Bars, 10 μm.

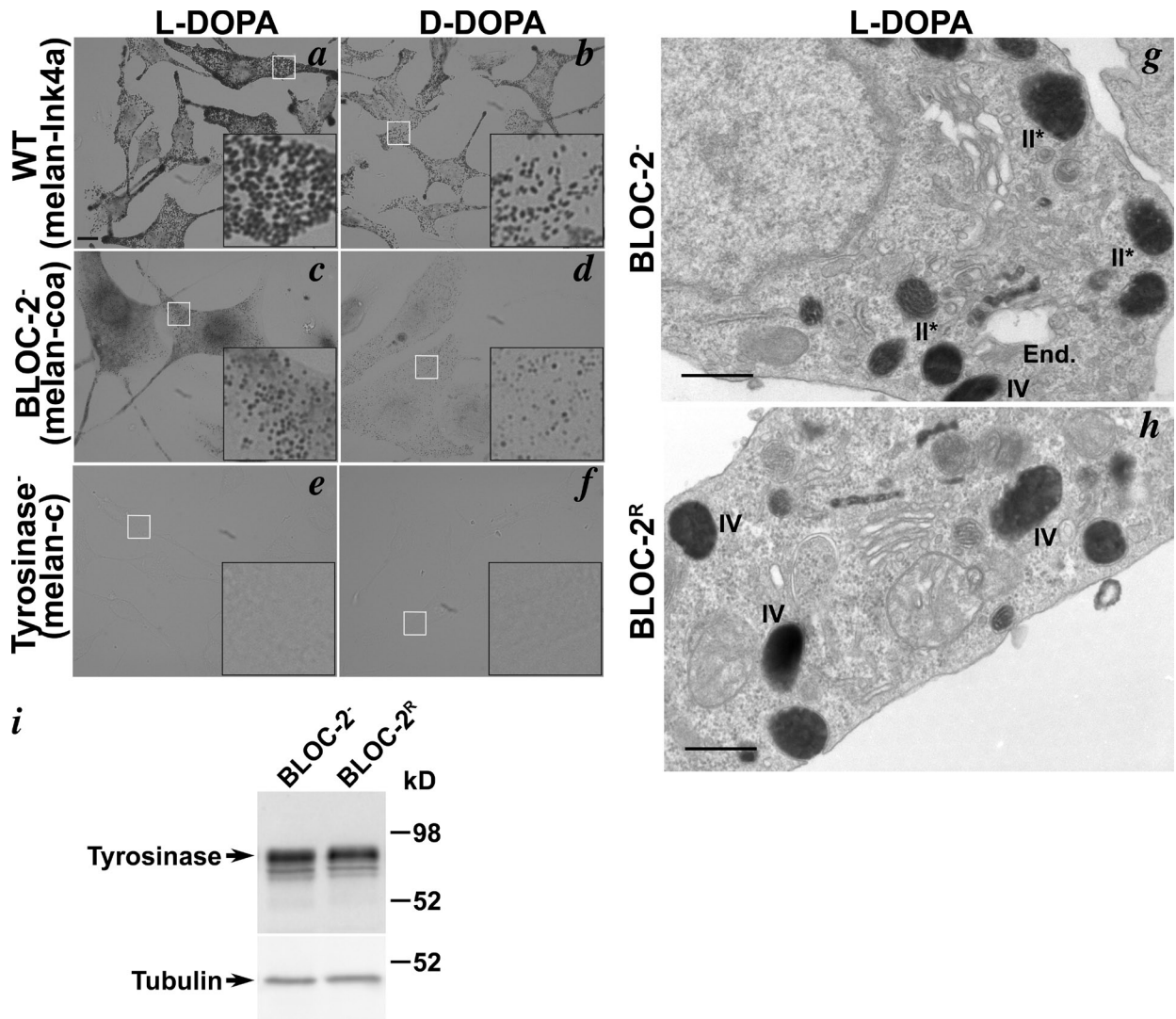


Figure S2. **BLOC-2⁻ cells retain substantial tyrosinase activity potential within melanosomes.** (a-h) Fixed WT (melan-Ink4a, a and b), BLOC-2⁻ (melan-coa, c, d, and g), TYR-deficient (melan-c, e and f), or BLOC-2^R (melan-coa:hHPS3, h) cells were treated with the TYR substrate L-DOPA or the control D-DOPA as indicated and then analyzed by bright-field microscopy (a-f; insets show 5x magnifications of boxed regions; bar, 10 μ m) or standard electron microscopy of thin sections (g and h; bars, 500 nm). TYR activity is indicated by increased pigment deposits in L-DOPA-treated cells. II*, pigmented stage II melanosomes; IV, stage IV melanosomes; End., endosome. (i) Whole cell lysates of BLOC-2⁻ and BLOC-2^R were fractionated by SDS-PAGE and immunoblotted with antibodies to TYR and to γ -tubulin as a loading control. Positions of molecular mass markers (in kilodaltons) are indicated to the right.

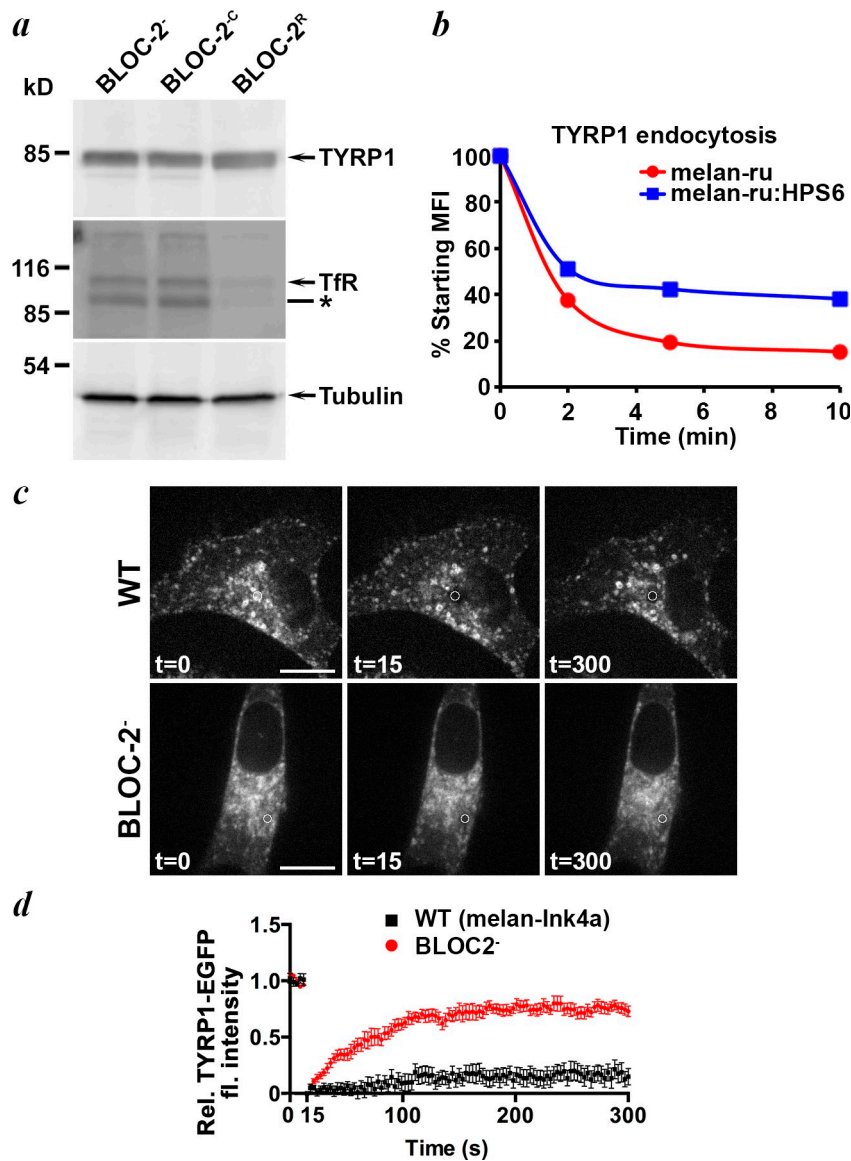


Figure S3. **Neither TYR1 expression levels nor endocytic rates are decreased in BLOC-2-deficient cells, but retrograde trafficking to the Golgi is enhanced.** (a) Whole cell lysates from BLOC-2^{-/-}, BLOC-2^{-C}, and BLOC-2^R cells were fractionated by SDS-PAGE and immunoblotted with antibodies to TYR1, TfR, or γ -tubulin as a loading control. Positions of molecular mass markers (in kilodaltons) is indicated to the left, and relevant bands are indicated by arrows to the right. The asterisk indicates the potential TfR degradation product. (b) TYR1 endocytosis rates were measured in BLOC-2-deficient melan-ru and “rescued” melan-ru:HPS6 cells as in Fig. 4 b. Values represent the percentages of mean fluorescence intensity (MFI) at each time point relative to that at time 0 from two separate experiments performed in duplicate. (c and d) WT melan-Ink4a or BLOC-2^{-/-} melanocytes stably expressing TYR1-EGFP were transiently transfected with GM130-mCh to mark the Golgi, pretreated with CHX for 60 min at 37°C, and then imaged by spinning-disk microscopy ($t = 0$). GFP fluorescence in a small region within the Golgi (white circles in c) was bleached at frame 5 ($t = 15$), and recovery of TYR1-EGFP fluorescence intensity was quantified over time by normalizing to prebleach GFP intensity of the same region in the same way as for whole Golgi FRAP in Fig. 6 (a–c). (c) Representative images for TYR1-EGFP from $t = 0$, $t = 15$, and $t = 300$ (300 s). Bars, 10 μ m. (d) Quantification of fluorescence recovery. Values represent the means \pm SD for GFP intensity traces of 15 cells of each type. Note the similarity for recovery in this experiment compared with the whole Golgi FRAP in Fig. 6 (a–c). Rel., relative; fl., fluorescence.

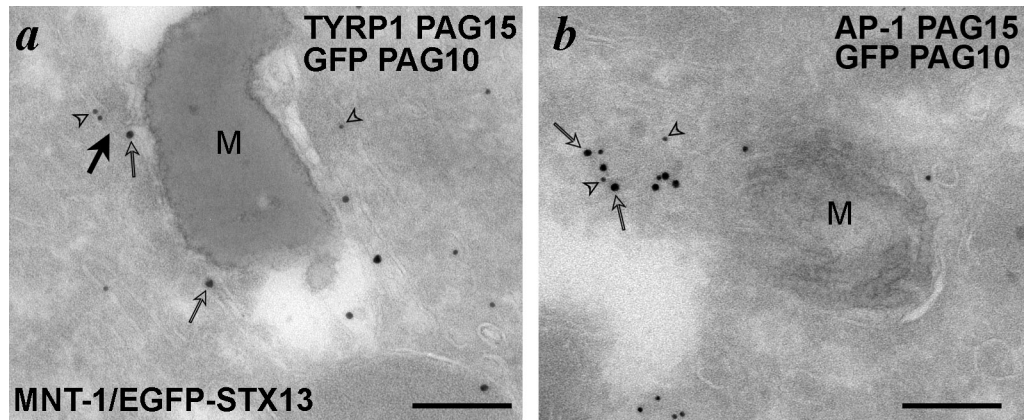


Figure S4. **EGFP-STX13 colocalizes with AP-1 and TYRP1 in tubulovesicular structures apposed to melanosomes.** (a and b) Immunoelectron microscopy analysis of ultrathin cryosections of fixed human MNT-1 melanoma cells that stably express EGFP-STX13. Sections were doubly labeled with anti-GFP antibody and protein A conjugated to 10-nm gold particles (PAG 10; open arrowheads), and either anti-TYRP1 (a) or anti- γ -adaptin (AP-1; b) antibodies and protein A conjugated to 15-nm gold particles (PAG15; open arrows). M, melanosome. Arrow (in a) points to a tubule that is adjacent to and/or continuous with the melanosome and that harbors both EGFP-STX13 and TYRP1. Bars, 200 nm.

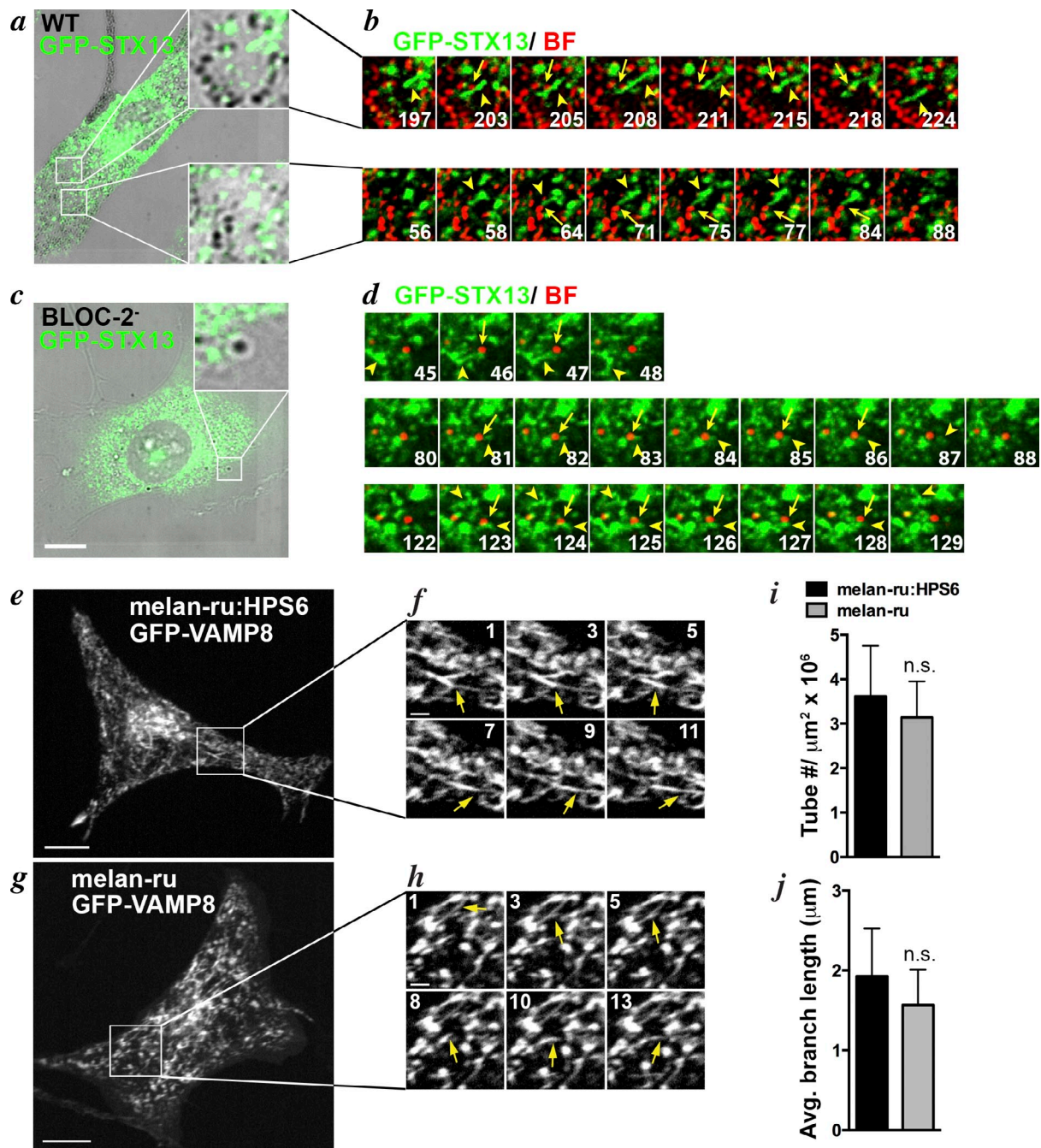
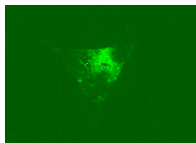
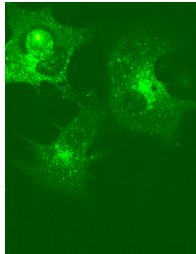


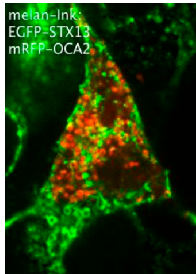
Figure S5. **BLOC-2 facilitates contacts of endosome-derived tubules with pigment granules but does not influence VAMP8-containing tubules.** (a–d). WT melan-*Ink4a* (a and b) and BLOC-2⁻ cells (c and d) stably expressing EGFP-STX13 were imaged in a single plane at 1 fps for 5 min by spinning-disk microscopy, alternating capture of bright-field (BF) and fluorescence images. (a and c) Frame from representative image series in which the fluorescence image is superimposed on the bright-field image. Boxed region is magnified 4x in inset. Bar, 10 μm. (b and d) Frames from the image series of the magnified boxed region in a and c at the times (seconds) indicated in lower right, in which the pigment granules observed by bright-field microscopy are pseudocolored red (after inversion of the image). Arrows, melanosomes that interact with tubules; arrowheads, examples of tubules. Note the extended interaction of a tubule with melanosomes in b but the much more transient interactions in d. (e–j). Transiently transfected “rescued” melan-*ru*:HPS6 (e and f) or BLOC-2–deficient melan-*ru* (g and h) expressing GFP-VAMP8 were imaged in a single plane by spinning-disk microscopy as in Fig. 7 and Fig. 8. Shown is a single frame (e and g) and an image sequence from the boxed region (3x magnified) taken over 11–13 s each (f and h) as indicated by the number at the top right (f) or left (h). The yellow arrow in each image sequence points to a single tubule observed in consecutive frames. Note the similar appearance of GFP-VAMP8–labeled tubes in both cell types. (i) The number of tubules per micrometer squared was quantified from 11 5-min (300 frame) acquisitions for each cell type covering the entire area of the cell. (j) After rendering by skeletonization as in Fig. 8 c, the mean branch length was measured for GFP-VAMP8 tubules in the same image sequences as in i. n.s., no significant difference. Bars, 10 μm.



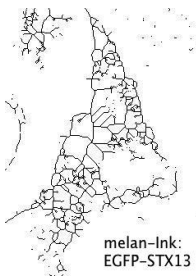
Video 1. **Recovery of TYRP1 fluorescence after photobleaching the Golgi in WT melanocytes.** WT melan-Ink4a melanocytes transiently transfected 24 h earlier with TYRP1-EGFP and GM130-mCh were treated with CHX for 60 min at 37°C and then imaged by spinning-disk confocal microscopy (UltraVIEW; PerkinElmer) for 2 min at 1 fps and an additional 3 min at one frame per 5 s. After 5 s (at frame 5), the Golgi was photobleached, and imaging was continued for 5 min. Image frames are shown at 7 fps. Images shown in Fig. 6 a are taken from this image sequence.



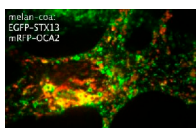
Video 2. **Recovery of TYRP1 fluorescence after photobleaching the Golgi in BLOC-2⁻ melanocytes.** BLOC-2⁻ melanocytes transiently transfected with TYRP1-EGFP and GM130-mCh were treated with CHX for 60 min at 37°C and then imaged by spinning-disk confocal microscopy (UltraVIEW; PerkinElmer) for 2 min at 1 fps and an additional 3 min at one frame per 5 s. After 5 s (at frame 5), the Golgi was photobleached, and imaging was continued for 5 min. Image frames are shown at 7 fps. Images shown in Fig. 6 b are taken from this image sequence.



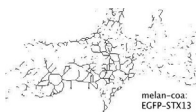
Video 3. **Fusion of endosomal tubules with melanosomes in WT melanocytes.** WT melan-Ink4a cells stably expressing EGFP-STX13 to mark early endosomes were transiently transfected with mRFP-OCA2 to mark melanosomes and then imaged by spinning disk confocal microscopy (UltraVIEW; PerkinElmer) for 5 min at 1 fps. Image frames are shown at 16 fps. An arrow at the start of the video denotes a mRFP-OCA2-labeled melanosome that interacts with multiple EGFP-STX13-containing endosomal tubules. Images shown in Fig. 8 (a and b, top) are taken from this image sequence.



Video 4. **Tubule formation by EGFP-STX13 in WT melanocytes.** EGFP-STX13 frames from Video 3 were converted into trajectories using the skeletonize function in ImageJ (<http://fiji.sc/Fiji>) to better appreciate the nature and dynamics of endosomal tubules.



Video 5. **Minimal fusion of endosomal tubules with melanosomes in BLOC-2⁻ melanocytes.** BLOC-2⁻ cells stably expressing EGFP-STX13 were transiently transfected with mRFP-OCA2 and then imaged by spinning-disk confocal microscopy (UltraVIEW; PerkinElmer) for 5 min at 1 fps as in Video 3. Image frames are shown at 16 fps. Images shown in Fig. 8 (a and b, bottom) are taken from this image sequence.



Video 6. **Tubule formation by EGFP-STX13 in BLOC-2⁻ melanocytes.** EGFP-STX13 frames from Video 5 were converted into trajectories using the skeletonize function in ImageJ (<http://fiji.sc/Fiji>) to better appreciate the nature and dynamics of endosomal tubules.

A source code for the MATLAB software used to quantify the interaction of EGFP-STX13 and mRFP-OCA2 in Fig. 8, modified from Jaqaman et al., 2008, is provided online as a ZIP file